Inert Gas Clusters Ejected from Bursting Bubbles during Sputtering

Klaus Franzreb and Peter Williams*

Department of Chemistry and Biochemistry, Arizona State University, Tempe, Arizona 85287, USA

(Received 19 December 2002; published 30 June 2003; publisher error corrected 2 July 2003)

Ar_n^+ cluster ions ($n \leq 6$) produced during prolonged Ar^+ ion surface bombardment of various sample materials at room temperature are shown to result from the ejection of neutral argon clusters following the rupture of high-pressure subsurface gas bubbles. Subsequent ion formation is shown to take place by resonant charge exchange with incident primary Ar^+ ions in the gas phase up to at least 175 μm above the surface. Xe_2^+ clusters are similarly produced from Xe^+-bombarded solids. The ion intensities of Ar_2^+ and Xe_2^+ are found to have a characteristic second-order dependence on primary Ar^+ or Xe^+ current density.

DOI: 10.1103/PhysRevLett.91.015501 PACS numbers: 61.80.Jh, 36.40.–c, 79.20.Rf, 82.30.Nr

High-dose ion implantation of gaseous species into solids can result in the accumulation of subsurface gas bubbles [1–3]. High-pressure inert gas bubbles in ion-implanted solids were predicted theoretically by Greenwood *et al.* in 1959 [1]. Transmission electron microscopy (TEM) images of He bubbles in α-irradiated Cu and Al were reported by Barnes and Mazey in 1960 [2]. A TEM study by Nelson in 1964 demonstrated for Ar^+ implanted Cu that the average size of Ar bubbles increases with elevated sample temperature [3]. Nelson noted similar behavior for He, Ar, and Xe bubbles in other metals after high-dose inert gas ion implantation. The pressure in inert gas bubbles roughly scales inversely with the radius [4,5] and can be high enough to form solid Ar and Xe at room temperature [5]. Ion beam sputtering leads to gas release due to rupture of the bubbles [3], producing a forward-directed flow with high kinetic energy. We show here that gas in this flow is cooled sufficiently to form weakly bound inert gas clusters.

Emission of ionized Ar_n^+ clusters from Ar^+-sputtered Al has indeed been detected [6–8], and fast neutral atom flows have been seen from Ar^+-sputtered Si [9,10]. However, there is disagreement about the origin of the fast neutral flows and there has been little discussion of the mechanism of formation of the ionized clusters. In this Letter we elucidate the emission and ion formation mechanisms leading to the observation of Ar_n^+ ($n \leq 6$) and Xe_2^+ from sputtered surfaces and show that these species arise from expansion cooling of gas from ruptured bubbles producing *neutral* clusters, followed by gas-phase ionization by resonant charge exchange. Laurent *et al.* in 1974 [6] first observed Ar_n^+ in a secondary ion mass spectrometry (SIMS) study of Ar^+-sputtered heated Al and noted that cluster ion formation must be due to rupture of bubbles during material removal by sputtering. Bernheim [7] suggested that formation of Ar_2^+ and Kr_2^+ might be due to autoionization of long-lived excited neutral Ar_2^* and Kr_2^* ejected from the Al surface, but he did not indicate how such highly excited dimers might be formed. In 1990, Katakuse *et al.* observed Ar_n^+ from Ar^+-bombarded Al without intentional sample heating [8] and again attributed this to sputter-induced rupture of bubbles, without referencing Laurent *et al.* [6] and without discussing the ion formation mechanism. Katakuse *et al.* also studied Xe^+-bombarded Al but did not report formation of Xe_n^+ [11].

Prior to Katakuse's work [8], a Dutch group [9,10] studied the angle-resolved energy distribution of Ar atoms reemitted from Ar^+-sputtered Si using electron impact ionization. Van Veen *et al.* observed two velocity components, one due to Ar gas thermally effusing from the surface, and a second, forward-peaked, with much higher energies attributed to gas expanding from ruptured bubbles [9]. Van Zwol *et al.* [10] refined the interpretation of [9] and attributed the second forward-peaked distribution to the directed Ar flow in a supersonic jet from ruptured bubbles. A Mach number of 1.6 was reported in [10] as a measure of associated jet cooling; it should be taken as a lower limit due to the microroughness of the sputtered surface which broadens the angular and velocity distributions. No attempt was made in [9,10] to detect Ar_n.

Feil *et al.* [12] later withdrew the interpretations of [9,10] and argued instead that the high-energy Ar flux resulted from ejected Ar atoms that had acquired kinetic energy in sputtering collision cascades. Feil *et al.* further suggested that the forward-peaked angular distributions of [9,10] were a result of the directional flow of Ar diffusing thermally to the surface [12]. This cannot be correct. First, there is no directed flow in diffusion, which is a random process. Second, for an Ar atom to participate in the sputtering collision cascade *and* to be ejected, it must initially reside at the surface within the sputtered atom escape depth. Up to ~85% of sputtered atoms originate in the outermost atomic layer and almost all the remainder originate from the second layer [13]. A simulation by Harrison [14] showed that Ar in a copper crystal is not stable against thermal ejection unless it is at least three layers deep. Thus the fraction of Ar ejected by a sputtering collision cascade is at most a few percent,

rather than the ~50% high-energy fraction reported in [9,10].

In this Letter we demonstrate that stable *neutral* Ar_n clusters are emitted from bursting Ar bubbles; ionized clusters are created by a subsequent charge-transfer process in the gas phase. A search for clusters of other inert gases (Xe, He) was also made. Cluster formation was studied for various materials: brittle semiconductors (Si, GaAs, Ge), soft and hard metals (Li, Mg, Al, Ti, Mo, Ta, Pb), and graphite. Positive ion data were obtained for steady-state sputtering in a Cameca IMS 3f secondary ion mass spectrometer. For Ar_n^+ studies, the targets were sputtered at room temperature by a mass-analyzed beam of $^{40}Ar^+$ (8 keV impact energy, ~2 μA current focused to ~100 μm diameter). Background pressure in the sample chamber was $\sim 3 \times 10^{-8}$ torr. The sample potential U could be varied over a few hundred volts around 4500 V. An important feature of the mass spectrometer is the fact that the strong ion accelerating field near the target surface (~ 1 V/μm) makes it possible to distinguish by energy analysis between ions ejected from the surface and ions formed in the gas phase in front of the target [15]. The accelerated ions passed through a 90° spherical sector electrostatic analyzer (ESA), set to transmit ions with kinetic energies of 4500 eV $\pm$ $\Delta E/2$. Depending on U, either secondary ions from the surface or ions formed in the gas phase in front of the target could pass through the ESA into the magnetic sector of the mass spectrometer. For example, for $U = 4500$ V, an ion formed 150 μm away from the target is accelerated through only 4350 V by the remaining extraction field and has not enough kinetic energy to pass through the ESA. To detect such an ion, U must be raised to ~4650 V so that this ion acquires a final kinetic energy of 4500 eV. Ion energy distributions were measured by step scanning U from 4425 to 4675 V with an energy bandpass $\Delta E \approx 5$ eV. Mass spectra were obtained at $U = 4650$ V and $\Delta E \approx$ 120 eV, corresponding to ions formed in the gas phase ~150 $\pm$ 60 μm in front of the surface.

Our study was stimulated by the observation of an intense $^{40}Ar_2^+$ signal at $m/z = 80$ in mass spectra of ^{40}Ar bombarded GaAs, using $U = 4650$ V to select ions formed above the sample. With a Cs^+ beam rather than Ar^+, no signal was seen at $m/z = 80$. An analysis of a variety of samples sputtered with Ar^+ under identical conditions ($U = 4650$ V) revealed similarly intense Ar_2^+ signals, ranging from ~1–4 $\times 10^4$ counts per second (c/s) for GaAs, Ge, Si, Mo, Ta, and Pb up to ~5–13 $\times 10^4$ c/s for Ti, Al, Mg, and Li, with the sole exception of C, where Ar_2^+ was not detectable. The atomic $^{40}Ar^+$ ion signal was nearly identical (~ 0.8–2×10^6 c/s) for all samples studied, including C. Figures 1(a) and 1(b) give two examples of such mass spectra for Mo and Ti. Besides Ar_2^+ at $m/z = 80$, the isotopic fingerprints of Mo^+ and Ti_2^+ are observed. Small signals due to doubly ionized dimers Mo_2^{2+} [16–18] were also seen and identified by their half-integer m/z values and isotopic

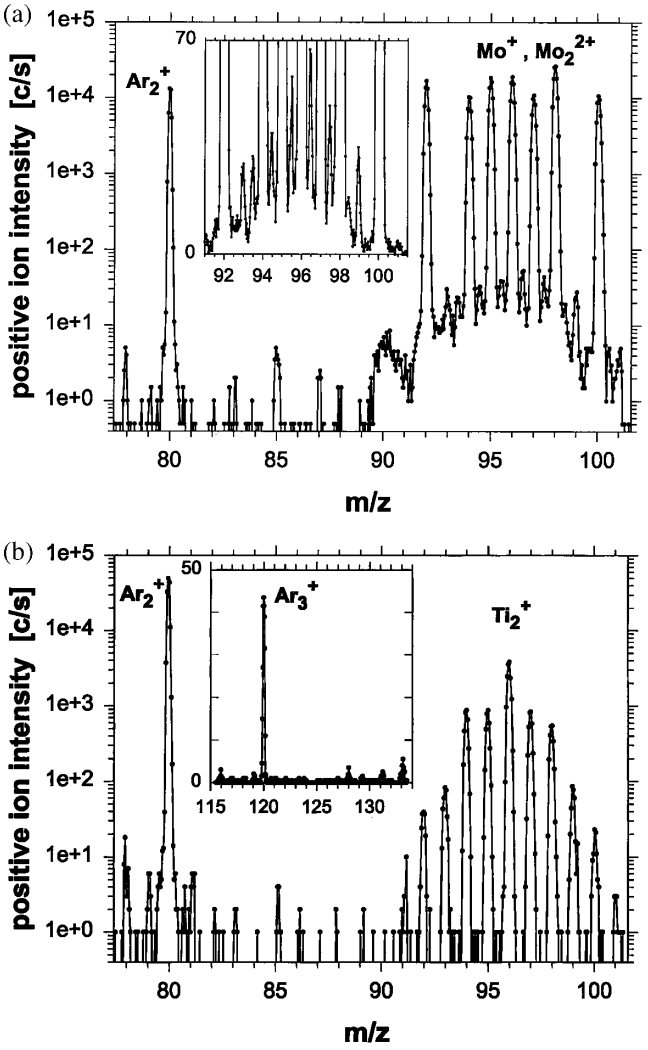

FIG. 1. (a) Mass spectrum of $^{40}Ar^+$ bombarded molybdenum foil obtained with a primary current of 2 μA at a sample potential of 4650 V ($\Delta E \approx 120$ eV; see text for details). Ions of $^{40}Ar_2^+$, Mo^+ as well as Mo_2^{2+} (inset) could be observed in the mass region shown. (b) Mass spectrum of a $^{40}Ar^+$ bombarded titanium target. Measurement conditions were identical to those used for (a). Ions of $^{40}Ar_2^+$, Ti_2^+, as well as $^{40}Ar_3^+$ (inset) could be observed in the mass regions shown.

abundance [linear inset in Fig. 1(a)]. $^{40}Ar_3^+$ at $m/z = 120$ was detected for Ti, as shown in the linear inset in Fig. 1(b). Ar_n^+ cluster ions with $3 \leq n \leq 6$ were observed only for Li, Mg, Al, and Ti targets. Cluster ions larger than Ar_6^+ or Xe_2^+ were beyond the mass range limitation of the mass spectrometer. Weak signals due to mixed clusters of Ar_mX^+ (X = Mg, Al, Ti) were also observed. The abundance distribution of Ar_n^+ is shown in Fig. 2. To our knowledge, Ar_n^+ production was previously only reported for an Al target [6–8]. The abundance patterns of Ar_n^+ for Al in [6], in [8], and in Fig. 2 are very different. In our room temperature study, Ar_2^+ is much more intense than bigger cluster ions. Laurent *et al.* state that the abundance distribution shifts to larger Ar_n^+ at elevated target temperature [6]. These differences most

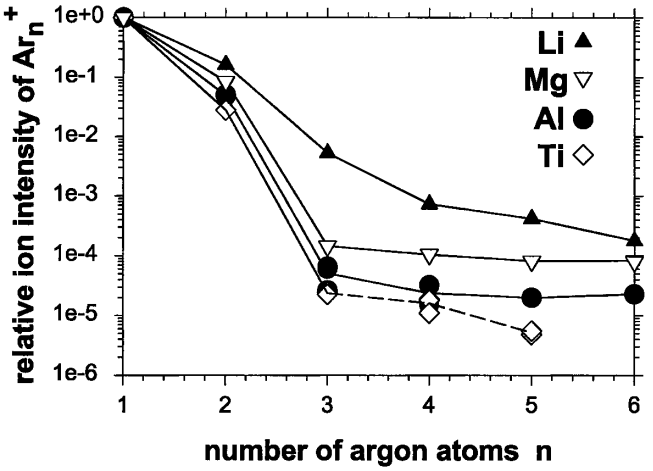

FIG. 2. Molecular argon ion abundance distributions of $^{40}Ar_n^+$ (normalized to the atom signal of $^{40}Ar^+$). Data are shown for $^{40}Ar^+$ bombarded Li, Mg, Al, and Ti metal targets analyzed at room temperature. Data were obtained for ions formed in the gas phase about 150 ± 60 μm in front of the sample surfaces.

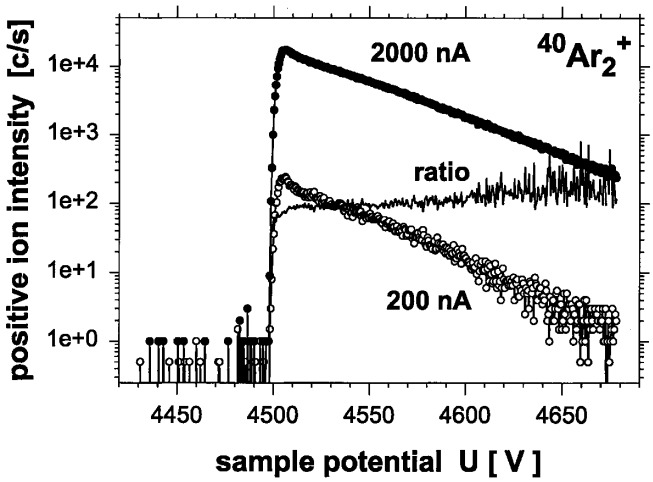

FIG. 3. Energy distributions of argon dimer ions of $^{40}Ar_2^+$ measured for a $^{40}Ar^+$ bombarded Ge wafer ($\Delta E \approx 5$ eV, see text for details). Ar_2^+ ions are formed exclusively in the gas phase in front of the sample surface. Data are shown for primary currents of 2000 and 200 nA, respectively. The corresponding intensity ratio is also shown and demonstrates a second-order dependence of Ar_2^+ signal on primary Ar^+ current density.

likely are due to the temperature dependence of the average Ar bubble size [3]. High-pressure, small bubbles form at room temperature while the faster argon diffusion at elevated temperature leads to formation of larger bubbles with a lower pressure [4–6]. Since the average size of small bubbles at room temperature is larger for softer materials [4,5] and the projected range of implanted Ar^+ is larger for lighter elements, our inability to observe Ar_n^+ with $n \geq 3$ in hard or in heavy materials suggests that larger clusters are formed only when Ar bubbles exceed a critical size and contain sufficient gas for a well-developed supersonic expansion to occur. In contrast, Ar_2^+ could be observed for all materials analyzed in this study, with the sole exception of C, and its formation does not seem to depend critically on material properties and bubble dimension. In carbon the high mobility of Ar diffusing between the graphitic carbon planes apparently allows Ar to escape rather than accumulate into bubbles.

The key to understanding the formation of Ar_n^+ is the measurement of ion energy distributions under conditions of a strong ion extraction field, together with the dependence of ion signal on primary Ar^+ current density J. Figure 3 shows the results of such a study for Ar_2^+ production from Ar^+ bombarded Ge. Ions sputtered from the sample surface with excess energies would appear at $U < 4500$ V; no signal above background ($\sim$1 c/s) is seen in this region. This shows that Ar_2^+ is *not* a sputtered ion. The usual explanation for ion signals at $U > 4500$ V is that the ions acquire their charge in the gas phase above the sample. We conclude that *neutral* Ar_2 therefore must have been emitted from the surface and remained intact over a distance of up to 175 μm prior to ionization. Energy distributions of Ar_3^+ and Ar_6^+ from Ar^+ bombarded Mg showed that ion formation of these two bigger clusters also takes place exclusively in the gas phase at a distance of up to 175 μm from the surface. Energy distributions confirmed that Ar^+ [7,19,20] and Ar^{2+} were also formed by gas-phase ionization of reemitted Ar atoms. Similarly, all of the other cluster species shown in Fig. 2 were detected as ions formed in the gas phase about 150 ± 60 μm in front of the sample surface.

Alternative explanations for the observation of energy-deficient Ar_2^+ clusters can be ruled out. Bernheim's suggestion of autoionization of long-lived highly excited states of emitted Ar_2^* [7] would require unusual lifetimes of several hundred nanoseconds, and so is unlikely to be correct. Energy-deficient ions could also result from in-flight dissociation of larger vibrationally excited cluster ions formed at the surface. Such larger cluster ions might nucleate on primary Ar^+ ions impacting, and being thermalized in, the initial high-pressure expansion from the ruptured bubbles; however, such a process should also produce Ar_2^+ directly and give rise to a peak at 4500 V sample potential. The absence of such a peak, and the identical shapes of the energy distributions for Ar^+ and Ar_2^+ show that such a process does not contribute significantly to the observed cluster ions. A three-body ($Ar^+ + Ar + Ar$) *associative* collision in the gas phase could form Ar_2^+ without the need of a preexisting Ar_2 parent or high-pressure bubbles and gas jets. The nonobservation of Ar_2^+ from C, when the reemitted total argon flux must have been identical to the other targets (and the Ar^+ ion signal *was* nearly identical) argues strongly against such association. Similarly, when Ar gas was admitted to the ion extraction region at a pressure sufficient to produce a gas density in front of the target

comparable to that resulting from ion bombardment and reemission, the Ar_2^+ signal from Ar^+ bombarded GaAs *dropped* by a factor of ~2.5, and disappeared completely when the Ar^+ beam was redirected into a small hole in the target holder. Also, increased collisional dissociation in this case should have *increased* the Ar_2^+ signal if this arose from dissociation of larger clusters.

The ionization process is presumed to be electron transfer between Ar_n and an incident primary Ar^+ ion (e.g., for $n = 2$, $Ar^+ + Ar_2 \rightarrow Ar + Ar_2^+$). Since the equilibrium internuclear distance is larger for neutral Ar_2, vertical ionization produces Ar_2^+ ions excited to high vibrational levels ($v' \sim 30$–40 [21]) in a process that is nearly resonant. Resonant capture can take place in a relatively distant collision without atomic momentum transfer, so that weakly bound Ar_n is not dissociated. Confirmation of this gas-phase ionization process comes from the determination of the current density dependence. Figure 3 shows the ratio of two energy spectra obtained at currents of 2000 and 200 nA for about the same Ar^+ beam size, i.e., for current densities J differing by a factor of 10. For Ar_2^+, and for Ar^+ and Ar^{2+}, over the entire energy range sampled, the signals varied almost exactly as the *square* of J; a reduction of J by a factor of 10 caused these ion energy distributions to be a factor of 100 less intense. Given any steady-state concentration of subsurface bubbles, the number of bubbles opened per unit time due to sputter erosion, and therefore the argon cluster flux, must be directly proportional to J. The ionization probability of Ar_2 is also directly proportional to J, leading to the observed J^2 dependence of the Ar_2^+ signal. The total argon flux leaving the surface at steady state is identical to the primary Ar^+ flux. Since the ionization probabilities of atomic Ar are proportional to J, the ion signals of Ar^+ and Ar^{2+} also scale with $\sim J^2$.

These findings are not restricted to argon. We also observed intense signals of the molecular isotopes of Xe_2^+ for Al and Si bombarded with Xe^+ (5.5 keV impact energy) at room temperature. Xe_2^+ was also ionized exclusively in the gas phase up to 175 μm above the surface, and also with a square dependence on J. The unique isotope signature for Xe^+ provided additional confirmation of the identity of Xe_2^+. An attempt to detect $^4He_2^+$ from a Si surface bombarded with a 75 nA $^4He^+$ beam at room temperature revealed a peak with a few counts/s intensity, but this signal increased dramatically when oxygen was admitted to the target region and was almost certainly due to formation of $^{16}O^{2+}$. $^4He_5^+$ was not detectable in a mass window free of possible interfering species at m/z 20. Observation of $^4He_2$ would be surprising because this dimer is very weakly bound, with a dissociation energy 5 orders of magnitude smaller [22] than those of Ar_2 (10.5 meV [21]) and Xe_2 (24 meV).

The Ar_2^+ data in Fig. 3 and analogous results for Xe_2^+ demonstrate that stable, ground-state *neutral* Ar_2 and Xe_2 are formed and survive in the gas phase up to at least 175 μm from the target surface prior to ionization. This corresponds to flight times of ≥ 0.3 μs for velocities ~500 m/s. The existence of such ejected neutral inert gas dimers and of larger Ar_n ($n \leq 6$) for Li, Mg, Al, and Ti is very strong evidence that supersonic expansion and cooling associated with rupture of high-pressure bubbles in vacuum is a general phenomenon. This explanation is consistent with all our experimental data and with the results by other groups [6–11] and provides a conclusive two-step mechanism to understand the emission and ionization of inert gas clusters from sputtered surfaces. Sputtering, e.g., of Li with 2 μA Ar^+ produces a steady-state flux of neutral Ar_n clusters consisting of $\sim 10^{13}$ Ar/s and roughly $\sim 10^{12}$ Ar_2/s and $\sim 10^{10}$ Ar_4/s. This process may be useful as an inexpensive *continuous* source of neutral inert gas clusters.

This work was supported by NSF Grant No. CHE 0111654. We thank Professor Georges Slodzian for informing us of the early work in his group, and Dr. Marc Bernheim for having provided us with a copy of his Ph.D. thesis. Erika Duda, Lynda Williams, and Rick Hervig also contributed to this work.

*Email address: pw@asu.edu

[1] G.W. Greenwood, A. J. E. Foreman, and D. E. Rimmer, J. Nucl. Mater. **1**, 305 (1959).
[2] R. S. Barnes and D. J. Mazey, Philos. Mag. **5**, 1247 (1960).
[3] R. S. Nelson, Philos. Mag. **9**, 343 (1964).
[4] H. Trinkaus, Radiat. Eff. Defects Solids **78**, 189 (1983).
[5] A. vom Felde *et al.*, Phys. Rev. Lett. **53**, 922 (1984).
[6] R. Laurent, G. Blaise, and G. Slodzian, C. R. Acad. Sci. B **278**, 11 (1974).
[7] M. Bernheim, Ph.D. thesis, Université de Paris–Sud centre d'Orsay, 1974, p. 99.
[8] I. Katakuse, H. Ito, and T. Ichihara, Int. J. Mass Spectrom. Ion Proc. **99**, 207 (1990).
[9] G. N. A. van Veen *et al.*, Phys. Rev. Lett. **57**, 739 (1986).
[10] J. van Zwol *et al.*, Appl. Surf. Sci. **43**, 363 (1989).
[11] Y. Saito, I. Katakuse, and H. Ito, Chem. Phys. Lett. **161**, 332 (1989).
[12] H. Feil *et al.*, Phys. Rev. B **43**, 13 695 (1991).
[13] D. E. Harrison, Jr., J. Appl. Phys. **52**, 4251 (1981).
[14] D. E. Harrison, Jr., *et al.*, in *Applications of Ion Beams to Metals*, edited by S. T. Picraux *et al.* (Plenum Press, New York, London, 1974), p. 427.
[15] P. Williams and L. A. Streit, Nucl. Instrum. Methods Phys. Res., Sect. B **15**, 159 (1986).
[16] T. T. Tsong, Surf. Sci. **177**, 593 (1986).
[17] F. Liu *et al.*, Phys. Rev. Lett. **59**, 2562 (1987).
[18] H. Ito *et al.*, Z. Phys. D **40**, 102 (1997).
[19] S. N. Schauer, R. Thomas, and P. Williams, Surf. Sci. **290**, 277 (1993).
[20] K. Franzreb *et al.*, Surf. Interface Anal. **26**, 597 (1998).
[21] T. Onuma *et al.*, J. Mol. Spectrosc. **198**, 209 (1999).
[22] R. E. Grisenti *et al.*, Phys. Rev. Lett. **85**, 2284 (2000).